Cellular/Molecular

17β-Estradiol Regulation of T-Type Calcium Channels in Gonadotropin-Releasing Hormone Neurons

Chunguang Zhang,[1]* Martha A. Bosch,[1]* Elizabeth A. Rick,[1] Martin J. Kelly,[1] and Oline K. Rønnekleiv[1,2,3]

[1]Department of Physiology and Pharmacology, [2]Department of Anesthesiology and Perioperative Medicine, and [3]Division of Neuroscience, Oregon National Primate Research Center, Oregon Health & Science University, Portland, Oregon 97239-3098

T-type calcium channels are responsible for generating low-threshold spikes that facilitate burst firing and neurotransmitter release in neurons. Gonadotropin-releasing hormone (GnRH) neurons exhibit burst firing, but the underlying conductances are not known. Previously, we found that 17β-estradiol (E2) increases T-type channel expression and excitability of hypothalamic arcuate nucleus neurons. Therefore, we used ovariectomized oil- or E2-treated EGFP (enhanced green fluorescent protein)–GnRH mice to explore the expression and E2 regulation of T-type channels in GnRH neurons. Based on single-cell reverse transcriptase-PCR and real-time PCR quantification of the T-type channel α_1 subunits, we found that all three subunits were expressed in GnRH neurons, with expression levels as follows: Cav3.3 $\geq$ Cav3.2 $>$ Cav3.1. The mRNA expression of the three subunits was increased with surge-inducing levels of E2 during the morning. During the afternoon, Cav3.3 mRNA expression remained elevated, whereas Cav3.1 and Cav3.2 were decreased. The membrane estrogen receptor agonist STX increased the expression of Cav3.3 but not Cav3.2 in GnRH neurons. Whole-cell patch recordings in GnRH neurons revealed that E2 treatment significantly augmented T-type current density at both time points and increased the rebound excitation during the afternoon. Although E2 regulated the mRNA expression of all three subunits in GnRH neurons, the increased expression combined with the slower inactivation kinetics of the T-type current indicates that Cav3.3 may be the most important for bursting activity associated with the GnRH/LH (luteinizing hormone) surge. The E2-induced increase in mRNA expression, which depends in part on membrane-initiated signaling, leads to increased channel function and neuronal excitability and could be a mechanism by which E2 facilitates burst firing and cyclic GnRH neurosecretion.

Introduction

Gonadotropin-releasing hormone (GnRH) neurons are known to secrete GnRH in a pulsatile manner. Since immortalized GnRH neurons (GT1-7 cells) in culture also exhibit pulsatile secretion and activity, it appears that pulsatility may be an inherent function of GnRH neurons (Funabashi et al., 2001; Herbison, 2006). Studies of GnRH neurons expressing enhanced green fluorescent protein (EGFP) have documented that these cells often fire in episodes of repetitive bursts (Suter et al., 2000b; Kuehl-Kovarik et al., 2002). However, currently it is not known how these bursts are generated in GnRH neurons, although depolarizing afterpotentials (DAPs) or afterdepolarizing potentials are proposed to be involved (Kuehl-Kovarik et al., 2002; Chu and Moenter, 2006). We reported previously in guinea pig (GP) that DAPs are associated with a T-type current in phasic firing vasopressin neurons (Erickson et al., 1993). Moreover, based on current-clamp and voltage-clamp recordings in a variety of neurosecretory hypothalamic neurons as well as in thalamic and cerebellar neurons, it appears that calcium T-type channels are important for burst firing (Huguenard and Prince, 1992; Erickson et al., 1993; Kim et al., 2001; Kelly and Wagner, 2002; Molineux et al., 2006; Qiu et al., 2006a).

Three pore-forming α_1 subunits of the T-type channels (Cav3.1, 3.2, and 3.3) have been cloned (Perez-Reyes et al., 1998; Lee et al., 1999), with the specific gating properties of T-type channels being dependent on the subunit composition (McRory et al., 2001; Chemin et al., 2002; Molineux et al., 2006). Importantly, channels expressing the Cav3.1 and 3.2 subunits exhibit similar characteristics, and compelling evidence suggests that these subunits are involved in short burst firing in thalamocortical relay neurons (Chemin et al., 2002). Channels expressing Cav3.3 have slower kinetics and contribute to sustained electrical activities of thalamic reticular and cerebellar Purkinje neurons (Chemin et al., 2002). All three subunits are expressed in the preoptic and basal hypothalamic regions (Qiu et al., 2006a; Bosch et al., 2009). However, in neurons of the hypothalamic paraventricular nucleus, Cav3.1 is the major subtype that mediates T-type calcium channel-dependent low-threshold spikes (LTSs) (Lee et al., 2008).

T-type calcium currents were first identified in subgroups of GnRH neurons in cultures derived from the olfactory pit regions of embryonic mice (Kusano et al., 1995). Subsequent studies in rats expressing EGFP–GnRH neurons revealed that these neurons also exhibited functional expression of T-type calcium channels (Kato et al., 2003). Moreover, both P/Q- and T-type channels were found to be developmentally regulated in that the

Received March 4, 2009; revised June 22, 2009; accepted July 20, 2009.

This work was supported by Public Health Service Grants NS43330, NS38809, and DK 68098.

*C.Z. and M.A.B. contributed equally to this work.

Correspondence should be addressed to either Dr. Martin J. Kelly or Dr. Oline K. Rønnekleiv, Department of Physiology and Pharmacology, L334, Oregon Health & Science University, 3181 Southwest Sam Jackson Park Road, Portland, OR 97239-3098, E-mail: kellym@ohsu.edu or ronnekle@ohsu.edu.

DOI:10.1523/JNEUROSCI.2962-09.2009

Copyright © 2009 Society for Neuroscience 0270-6474/09/2910552-11$15.00/0

corresponding currents became more robust after puberty, whereas they were barely detectable in neonatal animals (Kato et al., 2003). This was the first indication that these channels were potentially regulated by sex steroids in the CNS. Recent studies using GP as well as mouse models have found that both the mRNA expression and the current density and function of T-type calcium channels are increased in arcuate nucleus neurons in ovariectomized (OVX) animals treated with 17β-estradiol (E2) (Qiu et al., 2006a; Bosch et al., 2009).

Therefore, the current studies were initiated to explore the role and E2 regulation of T-type channels in mouse EGFP–GnRH neurons. The studies revealed that the expression of Cav3.1, Cav3.2, and Cav3.3 mRNAs are increased during the morning of E2-induced positive feedback. Cav3.3 is also elevated during the afternoon, whereas Cav3.1 and 3.2 are decreased. Concomitant with these dynamic changes in mRNA expression, T-type current density and rebound excitation were augmented in GnRH neurons from E2-treated animals. Our results indicate that Cav3.3 may be particularly important for the increased excitability of GnRH neurons during positive feedback.

Materials and Methods

Animal treatment and experimental procedures. All animal treatments described in this study are in accordance with institutional guidelines based on National Institutes of Health standards and were performed with institutional Animal Care and Use Committee approval. For the electrophysiology and single-cell reverse transcriptase-PCR (RT-PCR) experiments, transgenic female mice expressing EGFP under the control of the GnRH promoter (EGFP–GnRH) were used (Suter et al., 2000a). Animals were group housed until surgery, at which time they were housed individually. All animals were maintained under controlled temperature and photoperiod (21°C; 12 h light and 12 h darkness) and given access to food and water *ad libitum*. Adult 1.5- to 4-month-old females were OVX under ketamine/xylazine anesthesia (10/2 mg/kg, i.p.) and were implanted with SILASTIC capsules containing sesame oil or 6.2 μg of E2 in oil, which yields plasma E2 levels of 5.4 $\pm$ 1.7 and 25.4 $\pm$ 4.5 pg/ml, respectively (Zhang et al., 2009). Six to 7 d later, oil- and E2-implanted mice were either used as they were without further treatment and killed at zeitgeber time (ZT) 3–4 (low-E2 group) (Fig. 1*A*) or injected, respectively, with oil (50 μl) or estradiol benzoate (EB) (1 μg in 50 μl) and killed the following day at ZT 3–4 or at ZT 9.5–10.5 (high-E2 group) (Fig. 1*B*). This E2 treatment paradigm, which yields plasma E2 levels of 77.6 $\pm$ 10.6 pg/ml, was designed to induce a luteinizing hormone (LH) surge during the late afternoon before lights were turned off on the day after the injection (Bronson and Vom Saal, 1979). It is known that GnRH neuronal activity is increased in E2-treated animals during the afternoon before the LH surge (Christian et al., 2005). Therefore, both morning and afternoon experiments were done to explore potential differences in T-type subunit mRNA expression and T-type channel activity. In all instances, the uterus was removed and weighed as an additional measure of plasma steroid levels (Bronson and Vom Saal, 1979). There was no significant difference in uterine weights between the morning and afternoon.

In another set of experiments to evaluate the effects of the membrane estrogen receptor (mER) agonist STX on the mRNA expression of T-type calcium channel subunits in GnRH neurons, we adapted the experimental design used in guinea pig that induced an increase in Cav3.1 mRNA expression in the arcuate nucleus (Roepke et al., 2008). Adult female mice were OVX and allowed to recover for 4 d, at which time injections of propylene glycol (PPG) or STX (18 mg/kg) in PPG were initiated and injections were continued every other day until day 16. The animals were killed at ZT 3–4 on the day after the last injection (Fig. 1*C*). The uterus was removed, weighed, and compared with that of E2-treated animals.

Preparation of preoptic area–GnRH slices. Mice were killed by decapitation. The brain was rapidly removed from the skull and a block containing the diagonal band and preoptic area (DB-POA) with the majority of GnRH neurons was immediately dissected. The DB-POA block was

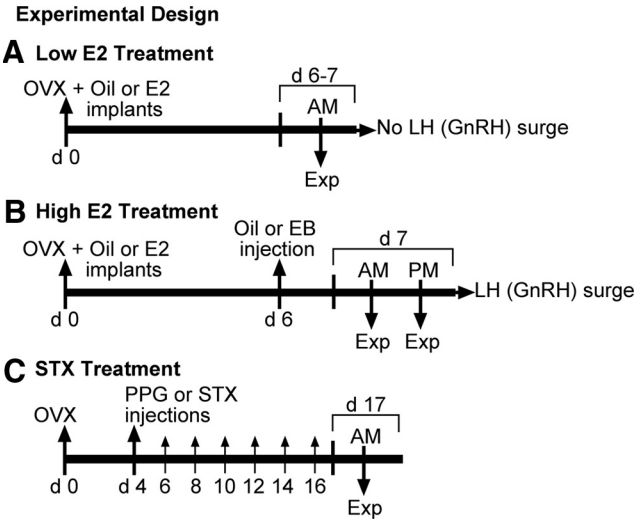

Figure 1. Experimental design. ***A***, Low-E2 group. Adult female mice were OVX and implanted with oil or E2 capsule on day 0. The animals were left to recover for 6–7 d, at which time they were used for experiments at ZT 3–4 (AM Exp). ***B***, High-E2 group. Adult female mice were ovariectomized and implanted with an oil or E2 capsule on day 0. The animals were left to recover for 6 d, at which time they were injected with oil or EB (1 μg) for induction of an LH (GnRH) surge the following day. The animals were killed on day 7 (d 7) at ZT 3–4 (AM Exp) or ZT 9.5–10.5 (PM Exp). ***C***, STX group. Adult female mice were OVX and allowed to recover for 4 d at which time vehicle (PPG) or STX injections were initiated and continued every other day until day 16. The animals were killed on day 17, the day after the last injection, at ZT 3–4. d 0, Day 0.

submerged in cold (4°C) oxygenated (95%O_2, 5% CO_2) high-sucrose artificial CSF (aCSF) consisting of the following (in mM): 208 sucrose, 2 KCl, 26 $NaHCO_3$, 10 glucose, 1.25 NaH_2PO_4, 2 $MgSO_4$, 1 $MgCl_2$, 1 $CaC1_2$, 10 HEPES, pH 7.4. Coronal slices (200–300 μm) from the DB-POA were cut on a vibratome during which time (10 min) the slices were bathed in high-sucrose aCSF at 4°C. The slices were then transferred to an auxiliary chamber in which they were kept at room temperature (25°C) in aCSF consisting of the following (in mM): 124 NaCl, 5 KCl, 2.6 NaH_2PO_4, 2 $MgSO_4$, 2 $CaCl_2$, 26 $NaHCO_3$, 10 HEPES, 10 glucose, pH 7.4, until recording (recovery for 2 h). A single slice at a time was transferred to the recording chamber, and each slice was kept viable by continually perfusing with warm (35°C), oxygenated aCSF at 1.5 ml/min.

Visualized whole-cell patch recording using epifluorescence and infrared-differential interference contrast videomicroscopy. Whole-cell patch recordings were made under a Carl Zeiss Axioskop FS outfitted with epifluorescence (FITC filter set) and infrared-differential interference contrast (IR-DIC) videomicroscopy. The area containing GnRH neurons was initially identified under low power (5× objective) with UV illumination (Fig. 2*A*). Then, the EGFP-tagged GnRH neurons (Fig. 2*B*) were visualized through a 40× water-immersion objective (Achroplan, Carl Zeiss), and their positions were marked on a monitor and compared carefully to their positions under IR-DIC imaging. Patch pipettes (A-M Systems; 1.5-mm-outer-diameter borosilicate glass) were pulled on a Brown/Flaming puller (Sutter Instrument; model P-97). Pipette resistances were 4–6 MΩ when filled with pipette solutions. In whole-cell configuration, access resistance was 10–20 MΩ. In a subset of the experiment to measure the activation or inactivation parameters of ion channels, the access resistance was <20 MΩ and was 80% compensated. Voltage-clamp experiments were performed with an Axopatch 1D amplifier (2 kHz low-pass filter, Axon Instruments).

Whole-cell recording of T-type calcium current. The T-type Ca^{2+} current was characterized in GnRH neurons from adult oil- and E2-treated ovariectomized female mice by using whole-cell patch recording. GnRH neurons have fewer dendrites than other CNS neurons, and we have been able to use whole-cell voltage clamp to isolate T-type current in GnRH, as well as arcuate pro-opiomelanocortin (POMC) and dopamine neurons. The effects of E2 treatment on the peak current, the peak current density, and the activation/inactivation (voltage and kinetic) characteristics of

T-type current were measured. For these analyses, the electrodes were filled with an internal solution consisting of the following (in mM): 100 Cs^+ gluconate, 20 tetraethylammonium-Cl, 10 NaCl, 1 $MgCl_2$, 10 HEPES, 11 EGTA, 4 ATP, 0.25 GTP; the pH was adjusted to 7.3 with CsOH at 300 mOsm. The voltage dependence was measured using standard protocols (see Fig. 7). To analyze the activation and inactivation kinetics of T-type channels in GnRH neurons, the channels were fully recovered (deinactivated) at −110 mV for 500 ms and were then activated at −50 mV for 500 ms. To pharmacologically verify that the calcium current is of the T type, we perfused with nickel (Ni^{2+}, 100–200 μM; Upjohn Pharmaceuticals) to block the current at the end of the recording. For measuring the role of the T-type calcium current on modulating cell firing characteristics and hence the effects of E2, we used a standard current-clamp protocol and a normal internal solution containing the following (in mM): 125 K^+-gluconate, 10 NaCl, 1 $MgCl_2$, 11 EGTA, 10 HEPES, 2 MgATP, 2 K_2ATP, 0.25 GTP. The cells were hyperpolarized to −100 mV (a level at which all of the T-type calcium channels are deinactivated) and then stepped back to the $V_{1/2}$ for activation (−55 mV) of T-type current. Subsequently, we measured the number of fast Na^+ spikes riding on the crest of the low-threshold spike (over a 1 s period). The hyperpolarization-recovered A-type and D-type potassium currents were blocked by 4-amino-pyridine (5 mM) and/or 2-aminoethyldiphenylborine (100 μM) (Wang et al., 2002). The Na^+ spikes were blocked by TTX to reveal the underlying LTS, and the LTS was abolished by Ni^{2+}.

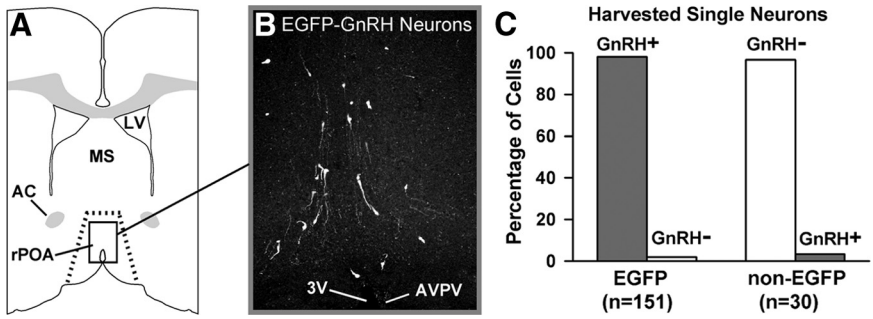

Figure 2. Slice dissection and GnRH neuronal distribution. ***A***, Schematic drawing of a rostral POA (rPOA) slice used for cell harvesting or whole-cell recording. The dotted line represents dissection used for dispersing and harvesting GnRH neurons. The boxed area (solid lines) is the area targeted for whole-cell recording of GnRH neurons. ***B***, Distribution of EGFP GnRH neurons within boxed area in ***A***. ***C***, Percentages of harvested EGFP GnRH neurons and non-EGFP neurons that express GnRH based on single-cell RT-PCR. 3V, Third ventricle; AC, anterior commissure; MS, medial septum; LV, lateral ventricle; AVPV, anteroventral periventricular nucleus.

Electrophysiology data analysis. The data were analyzed using p-Clamp Clampfit software (version 9.2, Molecular Devices). Subsequently, all electrophysiology data were transferred to GraphPad Prism 4 (GraphPad Software) or Sigma Plot 8.0 (Jandel Scientific) for statistical analysis and graphics (generation of figures). All values were expressed as mean ± SEM. Comparisons between two groups were made using an unpaired Student's *t* test or between multiple groups using a one-way ANOVA (with *post hoc* paired analysis). Differences were considered significant if the probability of error was <5%. Activation curves were fitted by the following Boltzmann equation: $I/I_{max} = 1/[1 + \exp[(V_{1/2} - V_s)/k]]$, where I is the peak current at step potential V_s, I_{max} is the peak current amplitude, $V_{1/2}$ is the step potential yielding half-maximum current, and k is the slope factor. Inactivation curves were fit with the following Boltzmann equation: $I/I_{max} = 1 - 1/[1 + \exp[(V_H - V_{1/2})/k]]$, where I is the peak current at step potential V_H, I_{max} is the peak current amplitude, $V_{1/2}$ is the step potential at which one-half of the current is inactivated, and k is the slope factor. The time constant of activation and inactivation of T-type current were obtained by fitting the currents with standard exponential function using the Clampfit software. The T-type currents were first fitted with one exponential (τ), but if they were not well fitted with one exponential, then two exponentials were used. The liquid junction potential was 10 mV, and all reported membrane potentials were corrected by subtracting 10 mV.

Cell harvesting of dispersed GnRH neurons and single-cell RT-PCR. Three or four 250 μm DB-POA slices were cut on a vibratome and placed in an auxiliary chamber containing oxygenated aCSF. The slices were allowed to recover for 1–2 h in the auxiliary chamber as described above. Thereafter, a discrete region of the organum vasculosum of the lamina terminalis (OVLT)-rostral POA was microdissected (Fig. 2*A*) and incubated in 10 ml of aCSF (pH 7.3, 300 mOsm) containing 1 mg/ml protease for ~17 min at 37°C. The tissue was then washed four times in low-calcium CSF (1 mM $CaCl_2$) and two times in aCSF. The cells were isolated by trituration with flame-polished Pasteur pipettes, dispersed onto a 60 mm glass-bottomed Petri dish, and perfused continuously with aCSF at a rate of 2.0 ml/min. The bipolar or unipolar fluorescent cells or adjacent cells were visualized using a Leica fluorescent microscope, patched, and then harvested by applying negative pressure to the pipette. In addition, five to six pools of five cells each were harvested from individual OVX oil- and E2-treated animals, as well as from PPG- and STX-treated animals, and expelled into siliconized microcentrifuge tubes. Each harvested cell or pool of cells was heat denatured and reverse transcribed as described previously (Zhang et al., 2007, 2008, 2009). Cells and tissue RNA used as negative controls were processed similarly but without RT.

Primers for the single-cell PCR were designed using the Clone Manager software (Sci Ed Software) and optimized for each reaction. The primers were as follows: mCav 3.1 (250 nt product, accession number NM_009783, forward primer 3013-3033 nt, reverse primer 3242-3262 nt); mCav3.2 (284 nt product, accession number NM_021415, forward primer 2640-2659 nt, reverse primer 2906-2923 nt); mCav3.3 (128 nt product, accession number NM_001044308, forward primer 965-983 nt, reverse primer 1076-1093 nt); mGnRH (239 nt product, accession number M14872, forward primer 21-40 nt, reverse primer 259-278 nt). In each case, the single-cell RT-PCR products were confirmed by sequencing. PCR was performed using 2–3 μl of cDNA template from each RT reaction in a 30 μl PCR mix as described previously (Zhang et al. 2007, 2008). Fifty cycles of amplification were performed using a DNA Engine Dyad Peltier thermal cycler (Bio-Rad) in 0.5 ml thin-walled PCR tubes according to the following protocols: 94°C for 2 min; 50 cycles of 94°C for 20 s, 56–60°C for 1 min, 72°C for 1 min; with a final 72°C extension for 5 min. Ten microliters of each PCR product was visualized with ethidium bromide on a 1.5% agarose gel. In addition to the controls described above, harvested aCSF in the vicinity of the dispersed cells was also used as a control in the RT-PCR. Using this method we found that >98% of EGFP harvested neurons (149 of 151) were GnRH-positive neurons, and similarly, >97% of non-EGFP neurons (29 of 30) were negative for GnRH (Fig. 2*C*).

Quantitative real-time PCR. Quantitative real-time PCR (qPCR) was performed on an Applied Biosystems (ABI) 7500 Fast real-time PCR system using the SybrGreen method for increased sensitivity (Zhang et al., 2008; Bosch et al., 2009). Primers were designed using the Clone Manager software and optimized for real-time PCR as described previously (Bosch et al., 2009). The primers were as follows: mCav 3.1 (144 nt product, accession number NM_009783, forward primer 2935-2954 nt, reverse primer 3059-3078 nt); mCav3.2 (84 nt product, accession number NM_021415, forward primer 2709-2728 nt, reverse primer 2773-2792 nt); mCav3.3 (128 nt product, accession number NM_001044308, forward primer 965-983 nt, reverse primer 1076–1093 nt); mβ-actin (63 nt product, accession number NM_007393, forward primer 849-867 nt, reverse primer 890-911 nt). The qPCR for Cav3.1, Cav3.2, Cav3.3, or β-actin contained 10 μl of Power SybrGreen 2× mastermix, 0.5 μM forward primer, 0.5 μM reverse primer, 2–4 μl cDNA, and nuclease-free water to a 20 μl final volume. qPCR was performed on samples in duplicate starting with a 10 min denaturation step at 94°C followed by 45 cycles of amplification at 94°C for 15 s (denaturation) and 60°C for 1 min (annealing) and completed with a dissociation step for melting point analysis which included 35 cycles of 95°C for 15 s, 60°C to 95°C in incre-

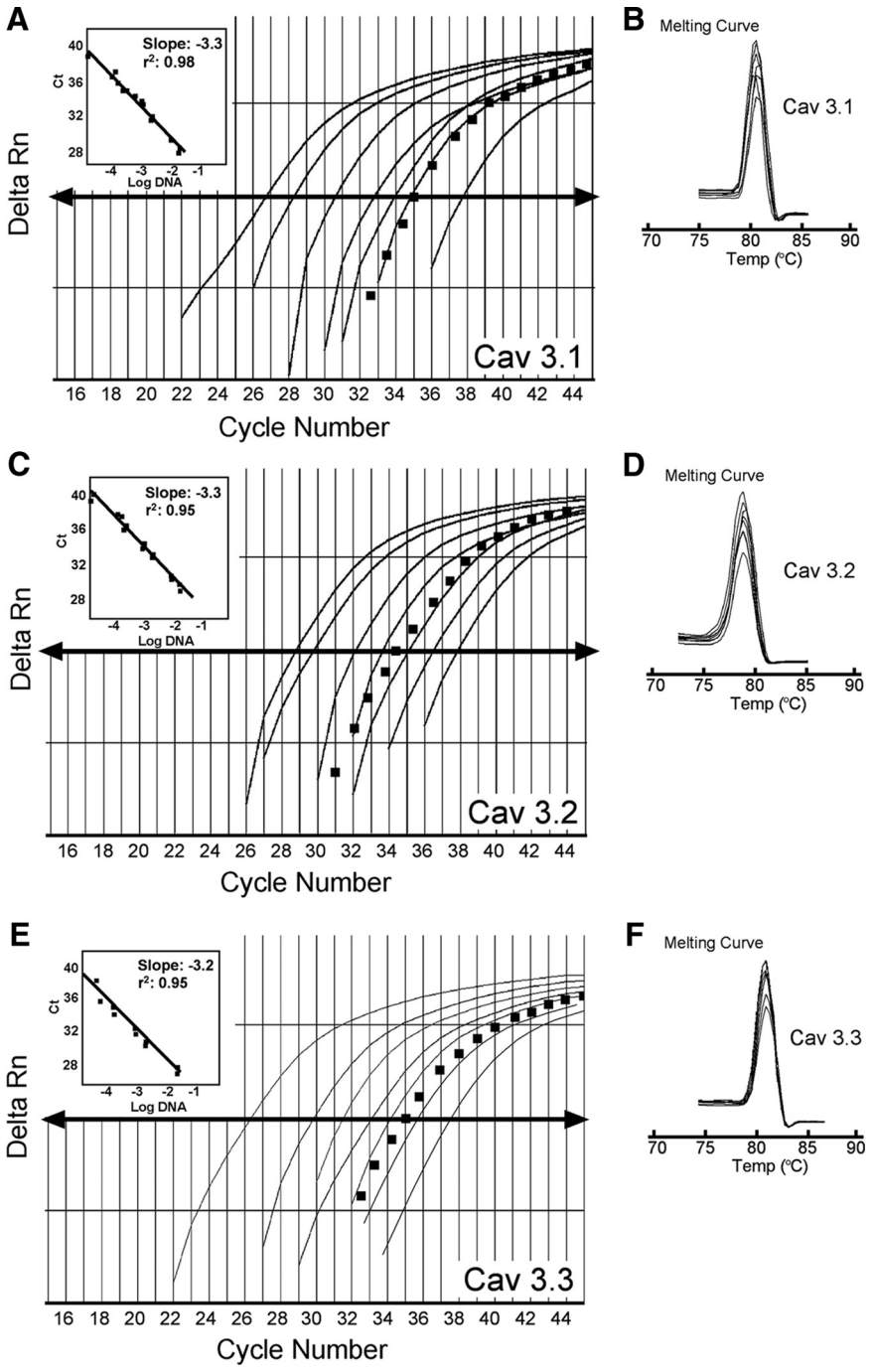

Figure 3. qPCR assays for Cav3.1 (α_1G), Cav3.2 (α_1H), and Cav3.3 (α_1I) transcripts using the SybrGreen method. ***A***, ***C***, ***E***, Standard curves were prepared with POA cDNA serial dilutions as follows: 1:50, 1:100, 1:500, 1:1000, 1:5000, 1:7000, 1:10,000. Cycle number was plotted against the normalized fluorescence intensity (Delta Rn) to visualize the PCR amplification. The cycle threshold (CT; arrow) is the point in the amplification at which the sample values were calculated. The POA cDNA serial dilutions and one representative GnRH pool (dotted line) are illustrated in ***A***, ***C***, and ***E***. ***B***, ***D***, ***F***, The superimposed dissociation (melting) curves for Cav3.1, Cav3.2, and Cav3.3 depict single-product melting at 80°C for Cav3.1 (***B***), 79°C for Cav3.2 (***D***), and 80.2°C for Cav3.3 (***F***). Single peaks illustrate that only one product was formed, and the lack of any other peaks illustrates that the primers did not form primer dimers. Insets in ***A***, ***C***, and ***E*** show standard curve regression lines and slopes from serial dilution data. The primer efficiencies calculated from the slopes were 100% for Cav3.1 and Cav3.2 and 96% for Cav3.3. β-Actin was used as control and its primer pair was also 100% efficient (data not shown). These efficiencies allowed us to use the $\Delta\Delta$CT method for quantification.

ments of 1°C for 1 min, and 95°C for 15 s. In all cases, real-time PCR assays were tested to determine and compare the efficiencies of the target and control gene amplifications. Serially diluted cDNAs from mouse POA, assayed in triplicate (Fig. 3), were used to construct standard curves and the efficiency was calculated according to the following formula: $E = 10^{(-1/m)} - 1$, where m is slope (Livak and Schmittgen, 2001; Pfaffl, 2001). Efficiencies were as follows: for Cav3.1, 100%; for Cav3.2, 100%; for Cav3.3, 96%; and for β-actin, 100%. The ABI sequence detection software system (version 1.3) was used to generate the standard curves (Fig. 3). The comparative $\Delta\Delta$CT method was used to calculate the individual values for each sample as described previously (Bosch et al., 2009). Briefly, the mean ΔCT of the vehicle-treated samples was used as an internal calibrator when comparing the mRNA quantities of Cav3.1, Cav3.2, and Cav3.3 in vehicle versus E2 or STX treatment. The relative linear quantity of the target gene was calculated using the formula $2^{-\Delta\Delta CT}$ (Livak and Schmittgen, 2001). Therefore, the data were expressed as an n-fold change in gene expression normalized to a reference gene (β-actin) and relative to a calibrator sample. The data are reported as relative mRNA expression.

Data analysis. For determination of GnRH neuronal expression of a particular transcript, 12–20 cells/animal were harvested from four oil-treated and five E2-treated mice, with totals of 74 and 77 cells, respectively. The number of cells expressing each transcript was counted for each animal and the mean number of neurons/animal was determined and used for further analysis of mean, SEM, and percentage expression. For quantification of expression differences between vehicle-treated ($n = 5$–6) and E2-treated ($n = 3$–6) or vehicle-treated ($n = 4$) and STX-treated ($n = 4$) animals, GnRH neuronal pools were analyzed using qPCR as follows: three to five pools of five cells each were analyzed from each animal, and the average mRNA expression in the neuronal pools was determined for each animal and used for further analysis of mean, SEM, and percentage expression. Student's t test was used to determine statistical significance ($p < 0.05$) between the normalized relative expression values.

Results

The mRNA expression of T-type calcium channel subunits is regulated by E2 in adult GnRH neurons

We previously reported that the T-type channel subunits Cav3.1, 3.2, and 3.3 are all expressed in the hypothalamus (Bosch et al., 2009). Since T-type channels are important for burst firing, we hypothesized that they would be expressed in GnRH neurons and play a role in the induction of the GnRH (LH) surge. To begin to address this question, we analyzed the mRNA expression of T-type calcium channel subunits in adult GnRH neurons. First, we used single-cell RT-PCR to measure the number of neurons expressing Cav3.1, Cav3.2, and Cav3.3 subunits in acutely dispersed GnRH neurons obtained during the morning from oil- and E2-treated mice. The three Cav3 subunits were found in subgroups of GnRH neurons, with expression levels as follows (in terms of the number of cells), regardless of treatment: Cav3.3 $\geq$ Cav3.2 $>$ Cav3.1 (Fig. 4). Since

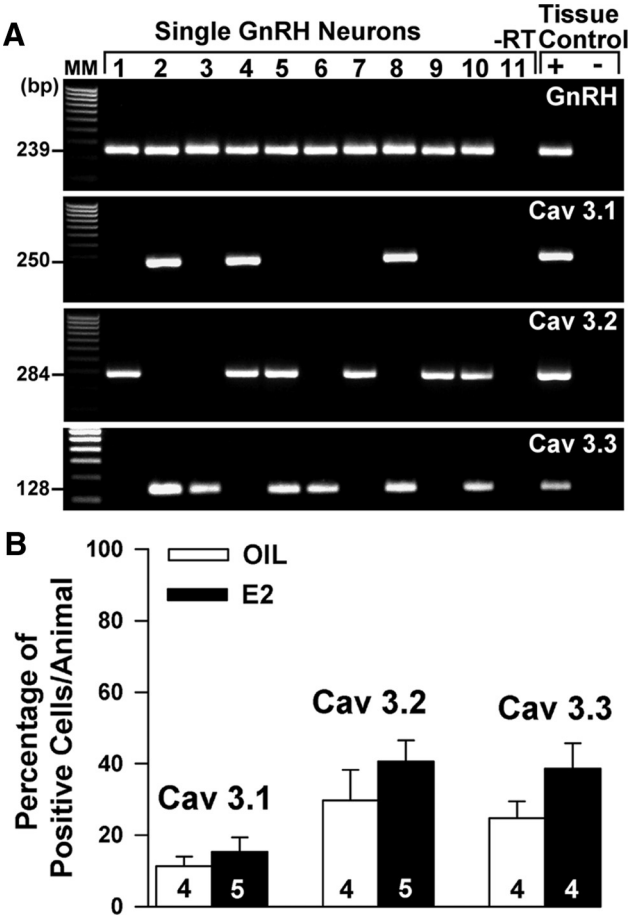

Figure 4. Cav3.1, Cav3.2, and Cav3.3 mRNA expression in single GnRH neurons. ***A***, Representative gel illustrating the mRNA expression of Cav3.1, Cav3.2, and Cav3.3 subunits in harvested GnRH neurons from E2-treated animals. The expected sizes of the PCR products are as follows (in base pairs): for GnRH, 239 bp; for Cav3.1, 250 bp; for Cav3.2, 284 bp, and for Cav3.3, 128 bp. Control GnRH neuron (−RT) was amplified from a harvested cell without reverse transcriptase. (A total of 8 neurons were processed without RT, all of which were negative). MM, Molecular marker. ***B***, Summary bar graphs of the percentages of expression of Cav3.1, Cav3.2, and Cav3.3 in GnRH neurons from oil- or E2-treated animals. Twelve to 20 GnRH neurons from each of 4 or 5 E2-treated and 12–20 neurons from each of 4 oil-treated females were analyzed, and the mean number of neurons expressing Cav3 subunits from each animal was used for further analysis. Bar graphs represent the mean ± SEM of percentage GnRH neurons expressing each Cav3 subunit/animal. Numbers of animals are indicated.

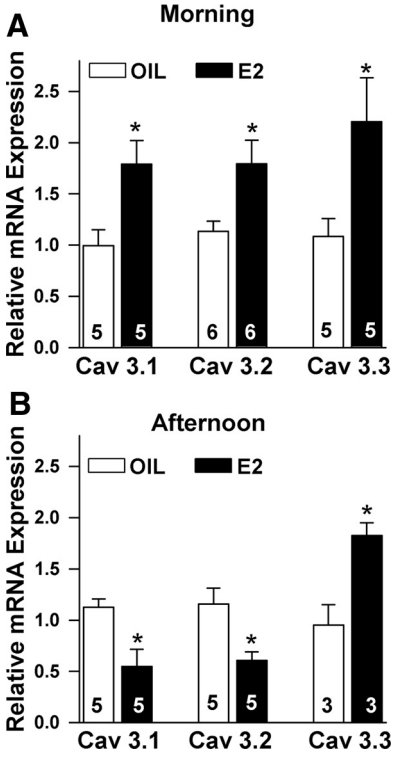

Figure 5. E2 regulates Cav3.1, Cav3.2, and Cav3.3 mRNA expression in GnRH neurons. ***A***, ***B***, Quantitative real-time PCR measurements of Cav3.1, Cav3.2, and Cav3.3 mRNAs in GnRH neuronal pools (3–5 per animal) from oil- and E2-treated mice ($n = 3–6$ animals per group) obtained during the morning (***A***) or during the afternoon (***B***). E2 upregulates the mRNA expression of Cav3.1, Cav3.2, and Cav3.3 during the morning. Cav3.3 remained high during the afternoon, but Cav3.1 and Cav3.2 were downregulated. The expression values were calculated via the ΔΔCT method and normalized to the mean ΔCT of the oil-treated samples. Bar graphs represent the mean ± SEM. *$p < 0.05$, oil versus E2.

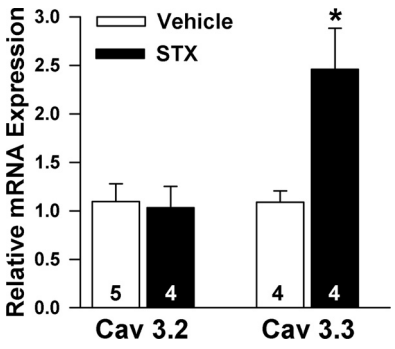

Figure 6. The mER agonist STX upregulates Cav3.3 mRNA expression in GnRH neurons. Quantitative real-time PCR measurements of Cav3.2 and Cav3.3 mRNAs in GnRH neuronal pools (3–5 per animal) from vehicle- and STX-treated mice ($n = 4–5$ per group) obtained during the morning. The expression values were calculated via the ΔΔCT method and normalized to the mean ΔCT of the vehicle-treated samples. Bar graphs represent the mean ± SEM. *$p < 0.05$, vehicle versus STX.

there was a trend for a greater number of cells expressing T-type channel subunits in E2-treated animals, we quantified Cav3.1, Cav3.2, and Cav3.3 mRNA expression in GnRH neuronal pools harvested during the morning (24 h postinjection) (Fig. 1*B*) from oil- and E2-treated animals. The GnRH pools were quantified using a SybrGreen real-time PCR assay that we had optimized for sensitivity and accuracy (Fig. 3). Indeed, we found that Cav3.1, Cav3.2, and Cav3.3 mRNAs were all significantly increased ($p < 0.05$) in GnRH neurons obtained from E2-treated animals during the morning (Fig. 5*A*). To evaluate whether T-type subunit mRNA expression would be further increased in E2-treated animals during the afternoon before the GnRH (LH) surge, GnRH neuronal pools harvested during the afternoon were also analyzed. Cav3.3 mRNA expression remained high in GnRH neurons during the afternoon ($p < 0.05$), but interestingly, Cav3.1 and Cav3.2 mRNA levels were both significantly reduced in the E2-treated compared with the oil-treated group during the afternoon ($p < 0.05$) (Fig. 5*B*). Therefore, our data show that the mRNA expression of all three T-type channel α_1 subunits were increased during the morning in response to elevated plasma E2 levels. Cav3.3 mRNA expression remained high during the afternoon, but Cav3.1 and Cav3.2 were both decreased during the afternoon immediately before the GnRH (LH) surge.

The mRNA expression of T-type calcium channel subunits is regulated by STX in adult GnRH neurons

We reported previously that female guinea pigs treated long term (3–4 weeks) with the mER agonist STX exhibited increased

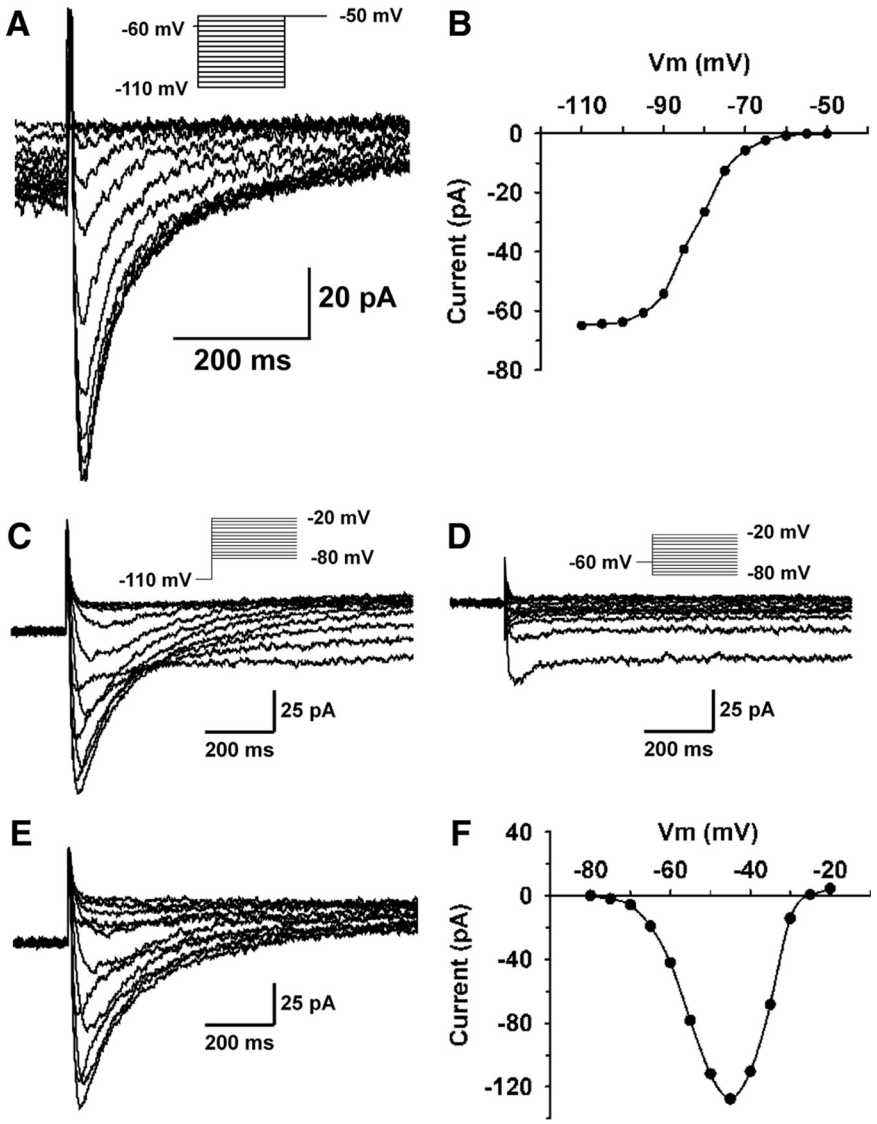

Figure 7. Characterization of the T-type calcium current expressed in GnRH neurons. ***A***, Hyperpolarization-dependent deinactivation of the T-type calcium channels. The T-type calcium channels were deinactivated at potentials from −50 mV to −110 mV for 500 ms before stepping to −50 mV to activate the current. The inset shows the voltage-clamp protocol. ***B***, The deinactivation *I–V* relationship of the T-type calcium channels obtained from ***A***. ***C***, Voltage dependence of low- and high-voltage-activated calcium channels. The insert shows the voltage-clamp protocol. ***D***, Voltage dependence of high-voltage-activated calcium channels. The insert shows the voltage-clamp protocol. ***E***, Voltage dependence of low-voltage-activated calcium channels obtained by subtracting values in ***D*** from those in ***C***. ***F***, Activation *I–V* relationship of the T-type calcium channels obtained from ***E***.

mRNA expression of Cav3.1 in the arcuate nucleus (Qiu et al., 2006b; Roepke et al., 2008), indicating that membrane-initiated signaling by E2 was involved in this response. To evaluate whether a membrane site of action was involved in the E2 regulation of T-type calcium channel subunits in GnRH neurons, we treated mice with STX or vehicle and measured Cav3.2 and Cav3.3 mRNA expression. We focused on Cav3.2 and Cav3.3, since these are the most prominent T-type channel subunits in GnRH neurons. The studies revealed that Cav3.3, but not Cav3.2, mRNA expression was significantly increased in GnRH neurons from animals treated with STX versus the vehicle (Fig. 6) ($p < 0.05$).

As reported previously with a lower dose of STX (Qiu et al., 2003), the current experiments also revealed that STX had no uterotropic effect. The uterine weights were 22.8 ± 1.6, 19.4 ± 1.3, and 102 ± 16.9 mg in vehicle-, STX- and E2-treated animals, respectively.

Intrinsic properties of adult GnRH neurons

The resting membrane potential in GnRH neurons of E2-treated females was more negative than that of oil-treated females [−62.5 ± 1.8 mV ($n = 14$) and −60.2 ± 1.4 mV ($n = 14$), respectively], supporting our previously published findings (Zhang et al., 2007). The input resistance did not differ between the oil- and E2-treated groups [1074 ± 133 MΩ ($n = 16$) and 919 ± 64 MΩ ($n = 14$), respectively]. In voltage clamp, prominent A-type potassium currents were recorded in 75% of GnRH neurons, regardless of the treatment, and 50% of the GnRH neurons expressed a hyperpolarization-activated (HCN) cation current (h-current), as previously reported (Zhang et al., 2007). Interestingly, the membrane capacitance (C_m) differed between the oil- and E2-treated morning groups [20.6 ± 0.8 pF ($n = 32$) versus 17.9 ± 0.7 pF ($n = 38$), respectively; $p < 0.05$], but there was no difference in C_m between the oil- and E2-treated afternoon groups [19.4 ± 0.7 pF ($n = 35$) versus 18.2 ± 0.9 pF ($n = 30$), respectively]. Regardless, whole-cell currents were expressed as current density (pA/pF) to normalize any differences in capacitance.

Characterization of T-type calcium currents in GnRH neurons

To evaluate the functional expression of T-type calcium channels in adult GnRH neurons, we performed whole-cell patch clamp recordings of GnRH neurons in slices from the DB/OVLT area (Fig. 2*A*,*B*). To obtain the deinactivation *I–V* relationship of the T-type calcium channels, the channels were deinactivated for 500 ms from −40 to −110 mV before stepping to −50 mV to activate the channels (Fig. 7*A*,*B*). The channels were completely deinactivated at potentials negative to −100 mV. To obtain the activation *I–V* relationship of the T-type calcium channels, the channels were deinactivated for 500 ms at −110 mV before stepping to a family of voltages (from −80 to −20 mV) to activate the T-type calcium channels (Fig. 7*C*). The total current obtained with this protocol also includes the high-voltage-activated (HVA) calcium currents. Therefore, the *I–V* relationship of the high-voltage-activated calcium channels was obtained by inactivating the T-type channels while deinactivating HVA calcium channels at −60 mV before stepping to a family of voltages (from −80 to −20 mV) to activate the HVA calcium channels (Fig. 7*D*). The net activation *I–V* relationship (Fig. 7*E*,*F*) of the T-type channels was obtained by subtracting the HVA *I–V* relationship (Fig. 7*D*) from the total current *I–V* relationship (Fig. 7*C*). Importantly, the T-type currents in GnRH neurons were attenuated

by nickel in a dose-dependent manner (Fig. 8). Moreover, the low-voltage- activated currents were not blocked by TTX, confirming previous findings (Qiu et al., 2006a). A T-type calcium current, characterized by its kinetics and pharmacological blockade by nickel, was recorded in nearly 100% of adult mouse GnRH neurons ($n = 136$).

To analyze the activation and inactivation kinetics of T-type channels in GnRH neurons, the channels were fully recovered (deinactivated) at −110 mV for 500 ms and then were activated at −50 mV for 500 ms. The activation curves of T-type current could be fitted with an exponential of 3–7 ms. The T-type currents in GnRH neurons showed three types of inactivation kinetics: fast, intermediate, and slow. The fast component could be fitted with an exponential of 30 ms, and the slow component could be fitted with an exponential of 200 ms. In those cells that exhibited only the slow component, their T-type currents could be well fitted with one component of 100–140 ms. Other cells could be fitted only with two exponentials, a fast τ of 30 ms and a slow τ of 200 ms. This would indicate that the T-type current expressed in GnRH neurons consists of multiple α_1 subunits with different kinetics. The fast inactivation kinetics would represent the expression of Cav3.1 and/or Cav3.2 subunits and the slow inactivation kinetics would represent the expression of Cav3.3 (Klockner et al., 1999; Chemin et al., 2002; Park et al., 2004).

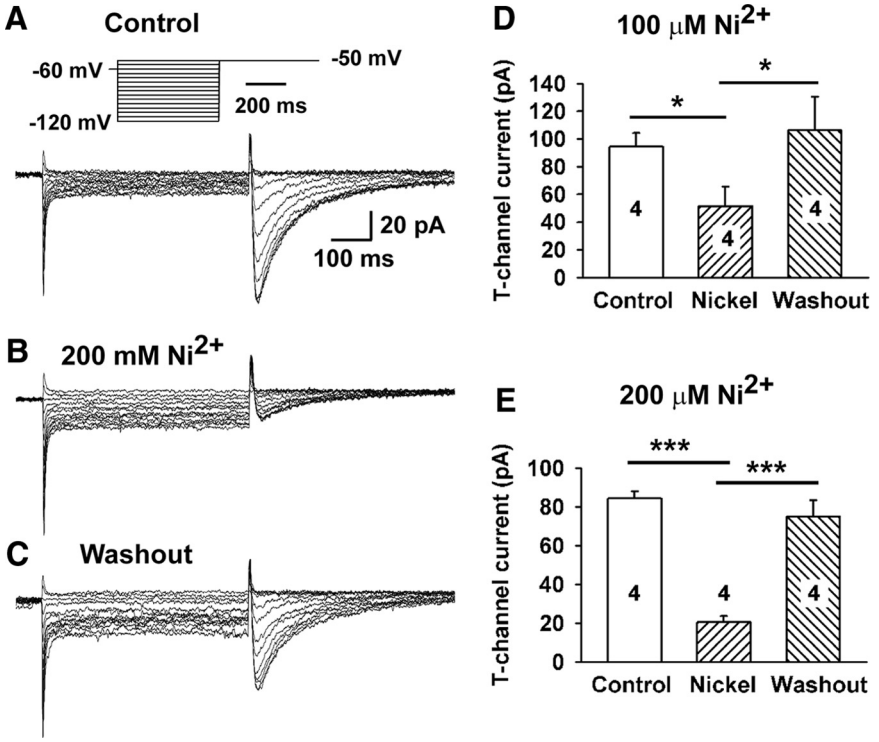

Figure 8. Nickel-sensitive T-type calcium currents are expressed in GnRH neurons. ***A–C***, T-type calcium current recorded from a GnRH neuron in control (***A***), with 200 μM Ni^{2+} (***B***), and after washout of Ni^{2+} (***C***). The inset in ***A*** shows the voltage-clamp protocol used to measure T-type calcium currents in GnRH neurons. ***D***, ***E***, Summary of the blockade of T-type currents expressed in GnRH neurons by Ni^{2+}. *$p < 0.05$, ***$p < 0.001$ (ANOVA). Numbers of cells are indicated.

T-type calcium currents are increased during the morning and afternoon of estradiol-induced positive feedback

To assess whether proestrous levels of E2 (>70 pg/ml) that increased the mRNA expression of T-type channel subunits in GnRH neurons translated into increased cell function, we measured the whole-cell T-type calcium currents in GnRH neurons in both OVX oil-treated animals and OVX E2-treated animals during the morning.

The studies revealed that the peak T-type current density was significantly increased during the morning ($p < 0.05$) in the E2-treated compared with the oil-treated group (Fig. 9*A*). In addition, the peak T-type current density was also increased during the afternoon in the E2-treated animals (Fig. 9*B*). Since there was no difference between morning and afternoon values in either the oil-treated or E2-treated groups, the morning and afternoon values were combined for each treatment group. This analysis further revealed that the T-type current density in GnRH neurons was significantly augmented in the E2-treated compared with oil-treated animals ($p < 0.01$) (Fig. 9*C*). Similar to our previous findings in guinea pig arcuate neurons (Qiu et al., 2006a), the deinactivation and activation curves of T-type channels were not affected by 17β-estradiol treatment (Fig. 9*D*). We determined that there was no difference in the voltage dependence of activation in cells from control vehicle-treated animals ($V_{1/2} = -53.4$ mV; slope factor, 1.05; $n = 40$) compared with cells from E2-treated animals ($V_{1/2} = -53.1$ mV; slope factor, 1.06; $n = 40$). Similarly, the voltage dependence of inactivation for control cells ($V_{1/2} = -80.4$ mV; slope factor, 1.01; $n = 40$) did not differ from that for E2-treated cells ($V_{1/2} = -80.7$ mV; slope factor, 1.01; $n = 40$). Interestingly, the window current (Fig. 9*D*) was small in GnRH neurons, an indication that these channels are relatively inactive at rest and may require a hyperpolarizing stimulus to deinactivate and recruit more T-type channels for burst firing.

It is well known that the T-type calcium channels underlie the LTSs, which are crucial for burst firing in many CNS neurons (Huguenard, 1996). Indeed, under current-clamp condition, E2 treatment, compared with oil treatment, increased the excitability of GnRH neurons as measured during the afternoon by the increased number of Na^+ spikes during rebound burst firing ($p < 0.05$) (Fig. 10). The h-currents measured at −100 mV were 2.7 ± 0.6 pA ($n = 10$) and 3.3 ± 1.0 pA ($n = 7$) in oil- and E2-treated GnRH neurons, respectively, resulting in a negligible sag in the membrane potential (Fig. 10). The remaining GnRH neurons from both groups of animals ($n = 6$ and 7, respectively) did not express an h-current. Therefore, since the h-current was small or absent, its contribution to the rebound firing was negligible.

T-type calcium currents are not increased by low diestrous levels of plasma E2

The T-type current density was measured also in GnRH neurons from animals treated with low diestrous levels of E2 (plasma levels of <30 pg/ml), levels that are sufficient to induce negative but not positive feedback (Fig. 1*A*) (Bronson and Vom Saal, 1979). Indeed, the peak T-type current densities were 4.42 ± 0.23

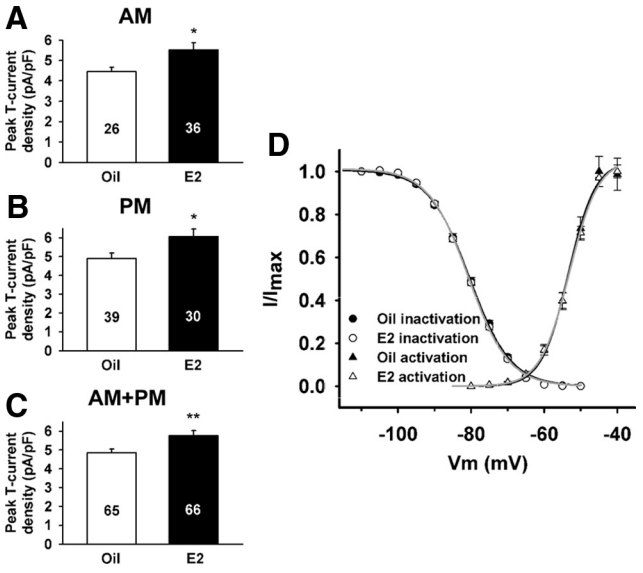

Figure 9. E2 treatment (positive-feedback regimen) increases the T-type calcium currents in GnRH neurons. ***A***, ***B***, E2 treatment increased the peak current density of the T-type calcium channels measured at either morning (AM) or afternoon (PM). *$p < 0.05$ (*t* test). Cell numbers are indicated. ***C***, Morning and afternoon data from ***A*** and ***B*** were combined. **$p < 0.01$ (*t* test). ***D***, *I–V* relationships of the activation and deinactivation of the T-type channels were not affected by E2 treatment. Deinactivation voltage was not affected by E2. $V_{1/2}$ and slope factor of deinactivation were -80.4 ± 0.2 mV and 1.01 ($n = 40$), respectively, in oil-treated cells versus -80.7 ± 0.2 mV and 1.01 ($n = 27$) for E2-treated cells. The activation voltage was also not affected by E2. $V_{1/2}$ and slope factor of activation were -53.4 ± 0.4 mV and 1.05 ($n = 40$), respectively, in oil-treated cells versus -53.1 ± 0.3 mV and 1.06 ($n = 27$) for E2-treated cells.

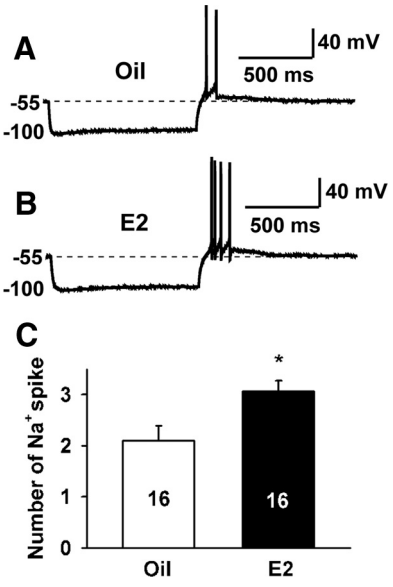

Figure 10. Functional E2-sensitive T-type calcium channels are expressed in GnRH neurons. ***A***, ***B***, Representative recordings showing the T-type calcium current-induced sodium spikes in oil-treated (***A***) or E2-treated (***B***) animals. In current-clamp mode, each cell exhibited an LTS, which triggered a burst of Na^+ action potentials after hyperpolarizing to -100 mV. Three to five trials were averaged for each cell. The rebound from the hyperpolarization evoked more Na^+ action potentials in GnRH neurons from E2-treated compared with oil-treated animals. ***C***, Summary of the effect of E2 treatment on the T-type current-induced sodium spikes. *$p < 0.05$ (*t* test). Numbers of cells are indicated.

pA/pF ($n = 22$) and 5.06 ± 0.65 pA/pF ($n = 22$) in oil- and E2-treated animals, respectively ($p > 0.05$). Therefore, low (diestrous) levels of E2 were not effective to increase T-type current density in GnRH neurons.

Discussion

For the first time, we show that the T-type calcium channel α_1 subunits, Cav3.1 (α_1G), Cav3.2 (α_1H), and Cav3.3 (α_1I), are all expressed in GnRH neurons, with Cav3.2 and Cav3.3 being the most prominent. Moreover, on the day of an E2-induced LH (GnRH) surge, the mRNA levels of the three channel subunits were significantly increased during the morning. Cav3.3 mRNA expression remained elevated during the afternoon, whereas Cav3.1 and Cav3.2 mRNA levels were reduced. The T-type current density was significantly enhanced during both the morning and afternoon with E2 treatment, and rebound excitation measured during the afternoon was also augmented. Therefore, the E2-dependent increase in T-type calcium channels may serve to augment the excitability of GnRH neurons in preparation for the GnRH (LH) surge.

The functional expression of T-type calcium channels in adult GnRH neurons has been controversial (Kato et al., 2003; Nunemaker et al., 2003). Using transgenic rats, Kato and coworkers have found, consistent with our results in the mouse, that the T-type calcium current is expressed in 100% of GnRH neurons after puberty. In contrast, Nunemaker et al. (2003) did not detect T-type current in adult mouse GnRH neurons. The reason for this discrepancy is not clear but could be attributable to differences in experimental design.

The expression of the T-type calcium channel α_1 subunits in GnRH neurons is consistent with our previous findings in other hypothalamic POA and arcuate nucleus neurons (Qiu et al., 2006a; Bosch et al., 2009). However, based on the number of neurons that we were able to detect, it appears that Cav3.3 and Cav3.2 are the most abundant in GnRH neurons, whereas the mRNA expression of Cav3.1 is less plentiful. This is different from what is seen for most other hypothalamic neurons (areas), in which Cav3.1 is more highly expressed (Lee et al., 2008; Bosch et al., 2009). The relatively slow inactivation of the T-type current in GnRH neurons is consistent with channels composed of Cav3.3 (α_1I) subunits (Klockner et al., 1999; Monteil et al., 2000; Chemin et al., 2002; Perez-Reyes, 2003; Park et al., 2004).

A major finding in this study is that the mRNA expression of all three α_1 subunits of T-type channels in GnRH neurons is already increased in E2-treated animals in the morning, but only Cav3.3 remained elevated during the afternoon at a time immediately before the LH (GnRH) surge. The increased expression during the morning with surge-inducing levels of plasma E2 fits with our previous findings both in the mPOA and in the arcuate nucleus (Qiu et al., 2006a; Bosch et al., 2009). However, it is well known that during proestrus or E2 treatment that mimics the proestrous phase of the ovulatory cycle, GnRH and LH levels are low during the morning, but a surge (supersecretion) of these hormones occurs during the afternoon before ovulation (Bronson and Vom Saal, 1979; Levine and Ramirez, 1982; Rønnekleiv and Kelly, 1988; Levine, 1997). In accordance with these findings, GnRH neuronal firing follows the same pattern with low firing activity during the morning and increased firing during the afternoon of the E2-induced LH surge, an indication of enhanced excitability (Christian et al., 2005). Our interpretation of the present data is that increased levels of E2 lead to increased T-type channel mRNA expression during the morning and subsequent increased excitability of GnRH neurons (Fig. 10). However, we propose that an E2-induced increased inhibitory input (e.g., GABA through $GABA_B$ receptors or E2-induced activation of K_{ATP} channels) during the morning *in vivo* would keep GnRH

neurons quiescent at this time point in spite of increased expression of T-type channels (Herbison, 2006; Zhang et al., 2007, 2009). During the afternoon, the E2-induced increase in Cav3.3 mRNA expression, T-type current density, and excitability combined with an E2-mediated excitatory (kisspeptin and possibly $GABA_A$) as well as a circadian input would augment cell firing and GnRH release (Pielecka-Fortuna et al., 2007; Clarkson et al., 2008; Zhang et al., 2008; Chappell et al., 2009). It is well known that in rodents the preovulatory GnRH and LH surges are entrained to the light/dark cycle through a circadian signal believed to reside in the suprachiasmatic nucleus (SCN) (Kalra, 1986; Levine, 1997; Christian and Moenter, 2008). Moreover, both *in vivo* and *in vitro* experiments have demonstrated that E2-induced GnRH secretion and the LH surge depend in part on input from the SCN, although the molecular mechanism is unknown (Rønnekleiv and Kelly, 1986, 1988; Ma et al., 1990; Levine, 1997; Funabashi et al., 2000; Chappell et al., 2009).

The T-type calcium currents contribute to burst firing of thalamic neurons (Huguenard and McCormick, 1992; Kim et al., 2001) but may also be important for burst firing of hypothalamic neurons and efficient release of neuropeptides including GnRH and vasopressin (Erickson et al., 1993; Fan et al., 2000; Kelly and Wagner, 2002). However, the activation of this crucial conductance is dependent on the membrane (hyper)polarization (Huguenard and McCormick, 1992; Kelly and Wagner, 2002), which is critical for removing the inactivation of T-type calcium channels (Fig. 9). Indeed, both GABA (via $GABA_B$ receptors) and opioids (via μ-opioid receptors) provide this critical input to GnRH neurons (Lagrange et al., 1995; Zhang et al., 2009). In addition, a hyperpolarizing stimulus would also activate a time-dependent HCN cation current (I_h or pacemaker current) that contributes to rhythmic firing and has been identified in GnRH neurons (Huguenard and McCormick, 1992; Lagrange et al., 1995; Ghamari-Langroudi and Bourque, 2000; Zhang et al., 2007). Furthermore, we believe that the membrane hyperpolarization generated by activation of inwardly rectifying potassium currents can set the stage for recruiting both the HCN and T-type calcium channels that are critical for phasic burst firing of GnRH neurons (Kelly and Wagner, 2002; Kuehl-Kovarik et al., 2002; Zhang et al., 2007, 2009).

The increased Cav3.3 mRNA expression during the afternoon as well as the slower channel inactivation kinetics would suggest that Cav3.3 T-type calcium channels are the most important for the increased activity (firing) associated with the GnRH/LH surge. GnRH neurons also exhibit a DAP, and the importance of the DAP for hypothalamic neuronal excitability has been well documented (Erickson et al., 1993; Ghamari-Langroudi and Bourque, 1998; Kuehl-Kovarik et al., 2005). Interestingly, Cav3.3 channels that are expressed in HEK cells are preferentially recruited during the DAP and can generate sustained activity, whereas the Cav3.1 and Cav3.2 currents promote short burst firing (Klockner et al., 1999; Kozlov et al., 1999; Chemin et al., 2002). Therefore, Cav3.3 T-type channels may be the major subtype for the sustained burst firing needed for the prolonged GnRH surge.

The mechanism by which E2 regulates the mRNA expression and function of T-type channels in GnRH neurons is not clear. We found previously that the E2-induced increase in Cav3.1 mRNA expression is dependent on ERα in the arcuate nucleus and the POA. In contrast, both ERα and ERβ can mediate the E2-induced increase in Cav3.2 (Bosch et al., 2009). Since ERβ is expressed in GnRH neurons, whereas ERα appears to be expressed presynaptically to GnRH neurons (Hrabovszky et al., 2000, 2001; Herbison et al., 2001; Kallo et al., 2001), the E2 regulation of Cav3.2 could be via ERβ. The following question remains: how are Cav3.1 and Cav3.3 regulated by E2 in GnRH neurons? An obvious possibility is that this could occur through E2-induced presynaptic inputs. Another possibility is that Cav3.1 and Cav3.3 mRNAs are regulated by a mER in GnRH neurons. Indeed, we now have compelling evidence that the mRNA expression of Cav3.3 is increased in GnRH neurons in females treated with the mER agonist STX. The diphenylacrylamide compound, STX, is a selective agonist for a mER and excites arcuate POMC neurons in an ERα/ERβ-independent manner (Qiu et al., 2003; 2006b). Therefore, T-type channel subunits in GnRH neurons similar to arcuate neurons could be regulated by E2 via a mER. However, the transcriptional effects of STX in GnRH neurons need to be further investigated.

In conclusion, we found that T-type calcium channel subunit expression and function are highly dependent on LH (GnRH) surge-inducing levels of E2. In addition, an E2-dependent diurnal signal appears to participate in the control of T-type channel subunit expression. Since the expression of T-type channels are crucial for neuronal burst firing, the E2-dependent regulation of T-type calcium channels could be a critical player in the ensemble of conductances that contribute to bursting activity in GnRH neurons and peptide release to ultimately ensure reproductive cyclicity.

References

Bosch MA, Hou J, Fang Y, Kelly MJ, Rønnekleiv OK (2009) 17β-Estradiol regulation of the mRNA expression of T-type calcium channel subunits: role of estrogen receptor α and estrogen receptor β. J Comp Neurol 512:347–358.

Bronson FH, Vom Saal FS (1979) Control of the preovulatory release of luteinizing hormone by steroids in the mouse. Endocrinology 104:1247–1255.

Chappell PE, Goodall CP, Tonsfeldt KJ, White RS, Bredeweg E, Latham KL (2009) Modulation of gonadotropin-releasing hormone (GnRH) secretion by an endogenous circadian clock. J Neuroendocrinol 21:339–345.

Chemin J, Monteil A, Perez-Reyes E, Bourinet E, Nargeot J, Lory P (2002) Specific contribution of human T-type calcium channel isotypes (alpha(1G), alpha(1H) and alpha(1I)) to neuronal excitability. J Physiol 540:3–14.

Christian CA, Moenter SM (2008) Vasoactive intestinal polypeptide can excite gonadotropin-releasing hormone neurons in a manner dependent on estradiol and gated by time of day. Endocrinology 149:3130–3136.

Christian CA, Mobley JL, Moenter SM (2005) Diurnal and estradiol-dependent changes in gonadotropin-releasing hormone neuron firing activity. Proc Natl Acad Sci U S A 102:15682–15687.

Chu Z, Moenter SM (2006) Physiologic regulation of a tetrodotoxin-sensitive sodium influx that mediates a slow afterdepolarization potential in gonadotropin-releasing hormone neurons: possible implications for the central regulation of fertility. J Neurosci 26:11961–11973.

Clarkson J, d'Anglemont de Tassigny X, Moreno AS, Colledge WH, Herbison AE (2008) Kisspeptin-GPR54 signaling is essential for preovulatory gonadotropin-releasing hormone neuron activation and the luteinizing hormone surge. J Neurosci 28:8691–8697.

Erickson KR, Rønnekleiv OK, Kelly MJ (1993) Role of a T-type calcium current in supporting a depolarizing potential, damped oscillations, and phasic firing in vasopressinergic guinea pig supraoptic neurons. Neuroendocrinology:789–800.

Fan YP, Horn EM, Waldrop TG (2000) Biophysical characterization of rat caudal hypothalamic neurons: calcium channel contribution to excitability. J Neurophysiol 84:2896–2903.

Funabashi T, Shinohara K, Mitsushima D, Kimura F (2000) Gonadotropin-releasing hormone exhibits circadian rhythm in phase with arginine-

vasopressin in co-cultures of the female rat preoptic area and suprachiasmatic nucleus. J Neuroendocrinol 12:521–528.

Funabashi T, Suyama K, Uemura T, Hirose M, Hirahara F, Kimura F (2001) Immortalized gonadotropin-releasing hormone neurons (GT1-7 cells) exhibit synchronous bursts of action potentials. Neuroendocrinology 73:157–165.

Ghamari-Langroudi M, Bourque CW (1998) Caesium blocks depolarizing after-potentials and phasic firing in rat supraoptic neurones. J Physiol 510:165–175.

Ghamari-Langroudi M, Bourque CW (2000) Excitatory role of the hyperpolarization-activated inward current in phasic and tonic firing of rat supraoptic neurons. J Neurosci 20:4855–4863.

Herbison AE (2006) Physiology of the gonadotropin-releasing hormone neuronal network. In: Knobil and Neill's physiology of reproduction, Ed 3 (Neill JD, ed), pp 1415–1482. Boston: Elsevier.

Herbison AE, Skynner MJ, Sim JA (2001) Lack of detection of estrogen receptor-α transcripts in mouse gonadotropin-releasing hormone neurons. Endocrinology 142:492–493.

Hrabovszky E, Shughrue PJ, Merchenthaler I, Hajszán T, Carpenter CD, Liposits Z, Petersen SL (2000) Detection of estrogen receptor-β messenger ribonucleic acid and ^{125}I-estrogen binding sites in luteinizing hormone-releasing hormone neurons of the rat brain. Endocrinology 141:3506–3509.

Hrabovszky E, Steinhauser A, Barabás K, Shughrue PJ, Petersen SL, Merchenthaler I, Liposits Z (2001) Estrogen receptor-beta immunoreactivity in luteinizing hormone-releasing hormone neurons of the rat brain. Endocrinology 142:3261–3264.

Huguenard JR (1996) Low-threshold calcium currents in central nervous system neurons. Annu Rev Physiol 58:329–348.

Huguenard JR, McCormick DA (1992) Simulation of the currents involved in rhythmic oscillations in thalamic relay neurons. J Neurophysiol 68:1373–1383.

Huguenard JR, Prince DA (1992) A novel T-type current underlies prolonged Ca^{2+}-dependent burst firing in GABAergic neurons of rat thalamic reticular nucleus. J Neurosci 12:3804–3817.

Kalló I, Butler JA, Barkovics-Kalló M, Goubillon ML, Coen CW (2001) Oestrogen receptor beta-immunoreactivity in gonadotropin releasing hormone-expressing neurones: regulation by oestrogen. J Neuroendocrinol 13:741–748.

Kalra SP (1986) Neural circuitry involved in the control of LHRH secretion: a model for preovulatory LH release. In: Frontiers in neuroendocrinology (Ganong WF, Martini L, eds), pp 31–75. New York: Raven.

Kato M, Ui-Tei K, Watanabe M, Sakuma Y (2003) Characterization of voltage-gated calcium currents in gonadotropin-releasing hormone neurons tagged with green fluorescent protein in rats. Endocrinology 144:5118–5125.

Kelly MJ, Wagner EJ (2002) GnRH neurons and episodic bursting activity. Trends Endocrinol Metab 13:409–410.

Kim D, Song I, Keum S, Lee T, Jeong MJ, Kim SS, McEnery MW, Shin HS (2001) Lack of the burst firing of thalamocortical relay neurons and resistance to absence seizures in mice lacking alpha(1G) T-type $Ca^{(2+)}$ channels. Neuron 31:35–45.

Klöckner U, Lee JH, Cribbs LL, Daud A, Hescheler J, Pereverzev A, Perez-Reyes E, Schneider T (1999) Comparison of the Ca^{2+} currents induced by expression of three cloned α1 subunits, α1G, α1H and α1I, of low-voltage-activated T-type Ca^{2+} channels. Eur J Neurosci 11:4171–4178.

Kozlov AS, McKenna F, Lee JH, Cribbs LL, Perez-Reyes E, Feltz A, Lambert RC (1999) Distinct kinetics of cloned T-type Ca^{2+} channels lead to differential Ca^{2+} entry and frequency-dependence during mock action potentials. Eur J Neurosci 11:4149–4158.

Kuehl-Kovarik MC, Pouliot WA, Halterman GL, Handa RJ, Dudek FE, Partin KM (2002) Episodic bursting activity and response to excitatory amino acids in acutely dissociated gonadotropin-releasing hormone neurons genetically targeted with green fluorescent protein. J Neurosci 22:2313–2322.

Kuehl-Kovarik MC, Partin KM, Handa RJ, Dudek FE (2005) Spike-dependent depolarizing afterpotentials contribute to endogenous bursting in gonadotropin releasing hormone neurons. Neuroscience 134:295–300.

Kusano K, Fueshko S, Gainer H, Wray S (1995) Electrical and synaptic properties of embryonic luteinizing hormone-releasing hormone neurons in explant cultures. Proc Natl Acad Sci U S A 92:3918–3922.

Lagrange AH, Rønnekleiv OK, Kelly MJ (1995) Estradiol-17β and μ-opioid peptides rapidly hyperpolarize GnRH neurons: a cellular mechanism of negative feedback? Endocrinology 136:2341–2344.

Lee JH, Daud AN, Cribbs LL, Lacerda AE, Pereverzev A, Klöckner U, Schneider T, Perez-Reyes E (1999) Cloning and expression of a novel member of the low voltage-activated T-type calcium channel family. J Neurosci 19:1912–1921.

Lee S, Han TH, Sonner PM, Stern JE, Ryu PD, Lee SY (2008) Molecular characterization of T-type Ca^{2+} channels responsible for low threshold spikes in hypothalamic paraventricular nucleus neurons. Neuroscience 155:1195–1203.

Levine JE (1997) New concepts of the neuroendocrine regulation of gonadotropin surges in rats. Biol Reprod 56:293–302.

Levine JE, Ramirez VD (1982) Luteinizing hormone-releasing hormone release during the rat estrous cycle and after ovariectomy, as estimated with push-pull cannulae. Endocrinology 111:1439–1448.

Livak KJ, Schmittgen TD (2001) Analysis of relative gene expression data using real-time quantitative PCR and the $2^{(-\text{delta-delta Ct})}$ method. Methods 25:402–408.

Ma YJ, Kelly MJ, Rønnekleiv OK (1990) Pro-gonadotropin-releasing hormone (ProGnRH) and GnRH content in the preoptic area and the basal hypothalamus of anterior medial preoptic nucleus/suprachiasmatic nucleus-lesioned persistent estrous rats. Endocrinology 127:2654–2664.

McRory JE, Santi CM, Hamming KS, Mezeyova J, Sutton KG, Baillie DL, Stea A, Snutch TP (2001) Molecular and functional characterization of a family of rat brain T-type calcium channels. J Biol Chem 276:3999–4011.

Molineux ML, McRory JE, McKay BE, Hamid J, Mehaffey WH, Rehak R, Snutch TP, Zamponi GW, Turner RW (2006) Specific T-type calcium channel isoforms are associated with distinct burst phenotypes in deep cerebellar nuclear neurons. Proc Natl Acad Sci U S A 103:5555–5560.

Monteil A, Chemin J, Leuranguer V, Altier C, Mennessier G, Bourinet E, Lory P, Nargeot J (2000) Specific properties of T-type calcium channels generated by the human α_{1I} subunit. J Biol Chem 275:16530–16535.

Nunemaker CS, DeFazio RA, Moenter SM (2003) Calcium current subtypes in GnRH neurons. Biol Reprod 69:1914–1922.

Park JY, Kang HW, Jeong SW, Lee JH (2004) Multiple structural elements contribute to the slow kinetics of the $Ca_V3.3$ T-type channels. J Biol Chem 279:21707–21713.

Perez-Reyes E (2003) Molecular physiology of low-voltage-activated t-type calcium channels. Physiol Rev 83:117–161.

Perez-Reyes E, Cribbs LL, Daud A, Lacerda AE, Barclay J, Williamson MP, Fox M, Rees M, Lee JH (1998) Molecular characterization of a neuronal low-voltage-activated T-type calcium channel. Nature 391:896–900.

Pfaffl MW (2001) A new mathematical model for relative quantification in real-time RT-PCR. Nucleic Acid Res 29:2002–2007.

Pielecka-Fortuna J, Chu Z, Moenter SM (2008) Kisspeptin acts directly and indirectly to increase GnRH neuron activity and its effects are modulated by estradiol. Endocrinology 149:1979–1986.

Qiu J, Bosch MA, Tobias SC, Grandy DK, Scanlan TS, Rønnekleiv OK, Kelly MJ (2003) Rapid signaling of estrogen in hypothalamic neurons involves a novel G protein-coupled estrogen receptor that activates protein kinase C. J Neurosci 23:9529–9540.

Qiu J, Bosch MA, Jamali K, Xue C, Kelly MJ, Rønnekleiv OK (2006a) Estrogen upregulates T-type calcium channels in the hypothalamus and pituitary. J Neurosci 26:11072–11082.

Qiu J, Bosch MA, Tobias SC, Krust A, Graham SM, Murphy SJ, Korach KS, Chambon P, Scanlan TS, Rønnekleiv OK, Kelly MJ (2006b) A G protein-coupled estrogen receptor is involved in hypothalamic control of energy homeostasis. J Neurosci 26:5649–5655.

Roepke TA, Xue C, Bosch MA, Scanlan TS, Kelly MJ, Rønnekleiv OK (2008) Genes associated with membrane-initiated signaling of estrogen and energy homeostasis. Endocrinology 149:6113–6124.

Rønnekleiv OK, Kelly MJ (1986) Luteinizing hormone-releasing hormone neuronal system during the estrous cycle of the female rat: effects of surgically induced persistent estrus. Neuroendocrinology 43:564–576.

Rønnekleiv OK, Kelly MJ (1988) Plasma prolactin and luteinizing hormone profiles during the estrous cycle of the female rat: effects of surgically induced persistent estrus. Neuroendocrinology 47:133–141.

Suter KJ, Song WJ, Sampson TL, Wuarin JP, Saunders JT, Dudek FE, Moenter SM (2000a) Genetic targeting of green fluorescent protein to gonadotropin-releasing hormone neurons: characterization of whole-cell electrophysiological properties and morphology. Endocrinology 141:412–419.

Suter KJ, Wuarin JP, Smith BN, Dudek FE, Moenter SM (2000b) Whole-cell recordings from preoptic/hypothalamic slices reveal burst firing in gonadotropin-releasing hormone neurons identified with green fluorescent protein in transgenic mice. Endocrinology 141:3731–3736.

Wang Y, Deshpande M, Payne R (2002) 2-Aminoethoxydiphenyl borate inhibits phototransduction and blocks voltage-gated potassium channels in *Limulus* ventral photoreceptors. Cell Calcium 32:209–216.

Zhang C, Bosch MA, Levine JE, Rønnekleiv OK, Kelly MJ (2007) Gonadotropin-releasing hormone neurons express K_{ATP} channels that are regulated by estrogen and responsive to glucose and metabolic inhibition. J Neurosci 27:10153–10164.

Zhang C, Roepke TA, Kelly MJ, Rønnekleiv OK (2008) Kisspeptin depolarizes GnRH neurons through activation of TRPC-like cationic channels. J Neurosci 28:4423–4434.

Zhang C, Bosch MA, Rønnekleiv OK, Kelly MJ (2009) $GABA_B$ receptor mediated inhibition of GnRH neurons is suppressed by kisspeptin-GPR54 signaling. Endocrinology 150:2388–2394.